ISSN XXXX XXXX © 2017 IJESC

Research Article Volume 7 Issue No.7

Maximum Power Point Tracking Wind Turbine Based on FOC Control of Variable Speed Axial Flux Permanent Magnet Synchronous Generator

Mohammed Kamal Ahmed
Assistant Professor
Department of Electrical Power and Machines
Faculty of Engineering, Al-Azhar University, Cairo, Egypt

Abstract:
This paper presents an innovative design of a low- speed, direct-drive axial flux permanent magnet generator (AFPMSG) for a wind turbine power generation system that is developed using mathematical and analytical methods, dynamic model of the axial flux generator developed using Simulink / MATLAB. A maximum power point tracking (MPPT)-based FOC control approach is used to obtain maximum power from the variable wind speed. The simulation results show the proper performance of the developed dynamic model of the AFPMSG, control approach and power generation system.

Index Terms: Axial Flux Permanent Magnet synchronous machines, Dynamic Model, MPPT

1.INTRODUCTION

Axial Flux Permanent Magnet (AFPM) synchronous machines have been growing in popularity and have received an increasing amount of attention in direct drive wind power application [1-3]. Depends on the flux flow in the air gap, the electromechanical energy conversion machines are categorized as Radial and Axial Flux Machines. The operating principle concerned with both the machines is alike but varies in its structure. The AFPMSG was designed with a single rotor, a double-sided air gap, and stators. The isotropic rotor is placed between teeth of the double-sided stators as shown in Fig. 1.

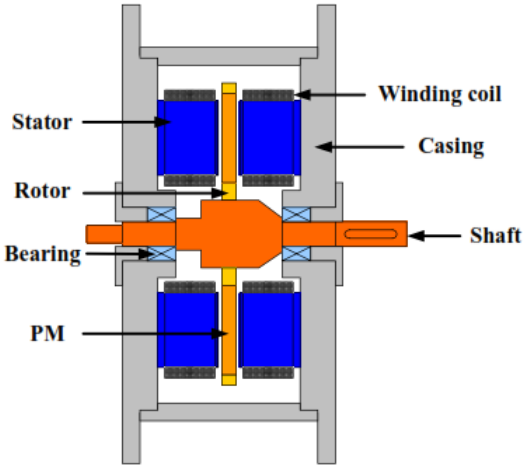

Figure.1. Cross section views of the AFPMSG

The stator back yokes are attached to the lateral case covers of the motor. The lateral case covers are made with rolled steel material. The stator teeth are individually fixed to the stator disk. The fan-shaped magnets of the rotor are mounted in holes of the rotor disk without the back yokes. Figure 2 shows the structure of the AFPMSG [1-4].

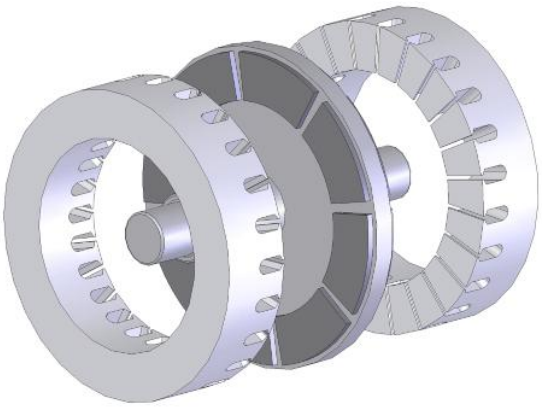

Figure.2.Magnetic circuit parts of an AFPMSG with one rotor-two-stators.

Figure 2 shows that the magnets are installed on both sides of the disc rotor so that the flux of a pole travels through both magnets associated with the pole. The main components of a direct-drive permanent magnet synchronous generator wind turbine are the wind turbine and the AFPMSG. The wind turbine captures the power from the wind for the system, and the AFPMSG transforms the mechanical power into electric power. In this paper, the principles of the electric power generation will be introduced, and the mathematical models of the wind turbine and the AFPMSG will be developed and analyzed. These will further help in understanding the control algorithms for the system as the following.

2. MODELING OF WIND TURBINES

In order to investigate the effectiveness of the energy conversion in wind energy conversion systems, first the available energy

stored in the wind needs to be determined. The wind turbine model is known as the aerodynamic model extracts power from the wind in the form of kinetic energy and then converts it into mechanical energy that is fed to the generator through a shaft. The aerodynamic power is given by to the following expression [7]:

$$P_m = \frac{1}{2} C_p(\lambda) \rho A U_w^3 \quad (1)$$

We shall use a generic equation of C_p as proposed by [8]. The equation is expressed below as:

$$C_p(\lambda, \theta) = 0.22\left(\frac{116}{\lambda_i} - 0.4\theta - 5\right) e^{-\frac{12.5}{\lambda_i}} + 0.0068\lambda_i \quad (2)$$

And $\frac{1}{\lambda_i} = \frac{1}{\lambda + 0.08\theta} - \frac{0.035}{1+\theta^3}$ (3)

The relationship between of Coefficient of power and Tip-speed ratio is given below.

The relationship between the tip-speed ratio λ and the rotor angular speed ω_m $(rads^{-1})$ is given as:

$$\omega_m = \frac{\lambda U_w}{R} \quad (4)$$

The relationship between the mechanical torque T_m and the mechanical power P_m is given by the equation below:

$$T_m = \frac{P_m}{\omega_m} \quad (5)$$

By subsisting P_m from (1) and ω_m from (4) into (5), the mechanical torque T_m is given as:

$$T_m = \frac{1}{2} C_t \rho A R U_w^2 \quad (6)$$

Where C_t is the torque coefficient and is given below as:

$$C_t = \frac{C_p}{\lambda} \quad (7)$$

Figure 3 shows The relationship between the Coefficient of power (Cp) versus Tip-speed ratio (lambda).The Simulik model of the wind turbine based on equations (1) to (7), is completed with the developed mechanical torque equation, is illustrated in Fig. (4).

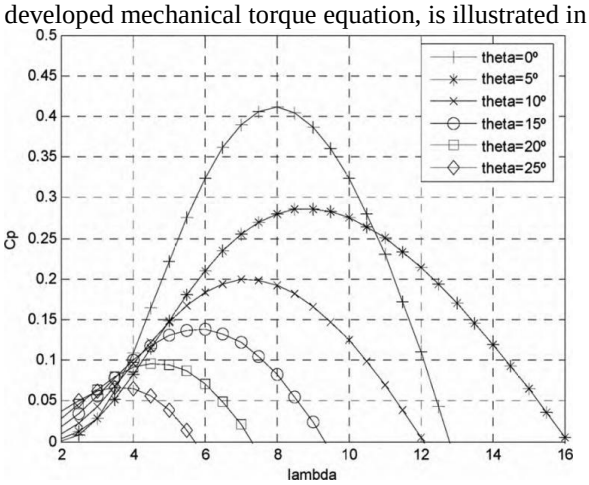

Figure.3. Coefficient of power (Cp) versus Tip-speed ratio (lambda)

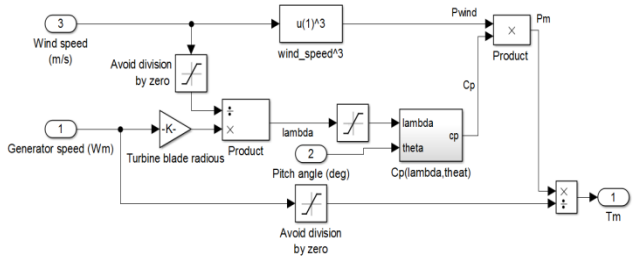

Figure.4. Wind turbine Simulink model.

3. MODELING OF PERMANENT MAGNET SYNCHRONOUS MACHINES

Permanent magnet synchronous machines/generators (PMSMs/AFPMSGs) play key role in direct-drive wind power generation systems for transforming the mechanical power into electrical power. A rigorous mathematical modeling of the AFPMSG is the prerequisite for the design of the machine control algorithms as well as the analysis of the steady-state and dynamic characteristics of wind energy conversion systems. The mathematical model of a AFPMSG in both the *abc*three-phase stationary reference frame and *dq*synchronously rotating reference frame will be developed, and the power and torque analysis of AFPMSGs will be given as well.

3-1 Modeling of a AFPMSG in the natural three-phase stationary reference frame

Before developing the mathematical model of the AFPMSG, several important assumptions need to be made:

(1) The damping effect in the magnets and in the rotor, are negligible;

(2) The magnetic saturation effects are neglected;

(3) The eddy current and hysteresis losses are neglected;

(4) the back electromotive force (EMF) induced in the stator windings are sinusoidal; (5) for simplicity, all the equations of AFPMSMs are expressed in motor (consumer/load) notation, that is, negative current will be prevailing when the model refers to a generator. Negative current means that at the positive polarity of the terminal of a device the current is out of that terminal. Figure 5 shows the Park transform for a three-phase AFPMSG generators. The fixed *abc*axes denote the direction of the MMFs (f_a,$f_b$and f_c) of the *a*, *b* and *c* phase windings, which are induced by the time varying three-phase AC currents in these stat or phase windings. The flux caused by the permanent magnet is in the direction of the *d*-axis fixed at the rotor. Here, the *d*-*q*-axes are rotating at the same angular speed of the PMs and rotor. Alsoθ_r , denotes the angle between the *d*-axis and the stationary *a*-axis.

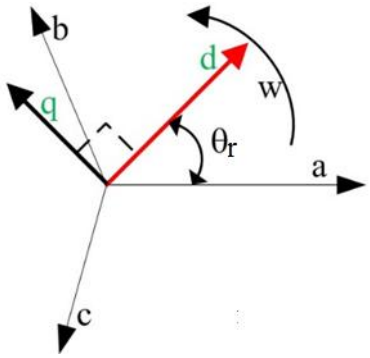

Figure.5. Park transform for AFPMSG generators.

The state space relationship of the terminal voltages of the AFPMSG to the phase currents and the phase flux linkages due to the PMs and stator currents can be written as follows [9]:

$$\begin{bmatrix} v_{as} \\ v_{bs} \\ v_{cs} \end{bmatrix} = \begin{bmatrix} R_s & 0 & 0 \\ 0 & R_s & 0 \\ 0 & 0 & R_s \end{bmatrix} . \begin{bmatrix} i_{as} \\ i_{bs} \\ i_{cs} \end{bmatrix} + \frac{d}{dt} \begin{bmatrix} \lambda_{as} \\ \lambda_{bs} \\ \lambda_{cs} \end{bmatrix} \quad (8)$$

Where,v_{as} , v_{bs}, and v_{cs} are the instantaneous *a*, *b*, and *c* three-phase stator voltages, andi_{as} , i_{bs}, and i_{cs} are the instantaneous

three-phase stator currents. Here,R_s is the statorwinding resistance per phase, and again, λ_{as},λ_{bs} , and $\lambda_{cs}$are the instantaneous flux linkages induced by the three-phase AC currents and the PMs, which can be expressed in expanded form as follows [9]:

$$\begin{bmatrix}\lambda_{as}\\ \lambda_{bs}\\ \lambda_{cs}\end{bmatrix}=\begin{bmatrix}L_{aa} & L_{ab} & L_{ac}\\ L_{ba} & L_{bb} & L_{bc}\\ L_{ca} & L_{cb} & L_{cc}\end{bmatrix}.\begin{bmatrix}i_{as}\\ i_{bs}\\ i_{cs}\end{bmatrix}+\begin{bmatrix}\lambda_r\cos(\theta_r)\\ \lambda_r\cos(\theta_r-\frac{2\pi}{3})\\ \lambda_r\cos(\theta_r+\frac{2\pi}{3})\end{bmatrix}(9)$$

where,L_{aa} , L_{bb}, and L_{cc}, are the self-inductances of the a, b, and c three-phases, and ,L_{ab}, L_{ac},L_{ba} ,L_{bc} ,L_{ca} and L_{cb} are the mutual inductances between these phases, while,λ_r , isthe rotor flux linkage caused by the permanent magnet. The self-inductances and mutual inductances are all functions of θ_r. Thus, all of the inductances are time varyingparameters.

3-2 Modeling of the AFPMSG in the dq-axes synchronously rotating reference frame

The *dq0* Park's transformation is a mathematical transformation which aims to simplify the analysis of synchronous machinery models, and was first introduced by R. H.Park in 1929 [10]. In the three-phase systems like PMSMs, the phase quantities which include stator voltages, stator currents, and flux linkages, are time varying quantities. By applying Park's transformation, which is in essence the projection of the phase quantities onto a rotating two axes reference frame, the AC quantities are transformed to DC quantities which are independent of time. The *abc*to *dq0* transformation can be expressed in matrix form as follows:

$$\begin{bmatrix}v_d\\ v_q\\ v_0\end{bmatrix}=\sqrt{\frac{2}{3}}\begin{bmatrix}\cos(\theta_r) & \cos(\theta_r-\frac{2\pi}{3}) & \cos(\theta_r+\frac{2\pi}{3})\\ -\sin(\theta_r) & -\sin(\theta_r-\frac{2\pi}{3}) & -\sin(\theta_r+\frac{2\pi}{3})\\ \frac{\sqrt{2}}{2} & \frac{\sqrt{2}}{2} & \frac{\sqrt{2}}{2}\end{bmatrix}(10)$$

The inverse Park's transformation is:

$$\begin{bmatrix}v_{as}\\ v_{bs}\\ v_{cs}\end{bmatrix}=\sqrt{\frac{2}{3}}\begin{bmatrix}\cos(\theta_r) & -\sin(\theta_r) & \frac{\sqrt{2}}{2}\\ \cos(\theta_r-\frac{2\pi}{3}) & -\sin\left(\theta_r-\frac{2\pi}{3}\right) & \frac{\sqrt{2}}{2}\\ \cos(\theta_r+\frac{2\pi}{3}) & -\sin(\theta_r+\frac{2\pi}{3}) & \frac{\sqrt{2}}{2}\end{bmatrix}(11)$$

In expressions (10) and (11), and can represent the stator voltages, stator currents or flux linkages of the AC machines, respectively. Considering that underbalanced conditions, v_0=0, the voltage function of the AFPMSG in the *dq*-axes reference frame can be expressed as follows [9]:

$$v_{ds}=R_s i_{ds}+L_d\frac{di_{ds}}{dt}-\omega_e L_q i_{qs}(12)$$

$$v_{qs}=R_s i_{qs}+L_q\frac{di_{qs}}{dt}+\omega_e L_d i_{ds}+\omega_e\lambda_r(13)$$

Where,v_{ds} and v_{qs}, are the instantaneous stator voltages in the *dq*-axes reference frame, andi_{ds} and i_{qs}, are the instantaneous stator currents in the *dq*-axes reference frame. Here,$L_d$and L_q, are the *d*-axis and *q*-axis inductances, and $\omega_e$is the electrical angular speed ofthe rotor, while, λ_r, is the peak/maximum phase flux linkage due to the rotor-mounted PMs. According to expressions (12) and (13), the equivalent circuits of the AFPMSG inthe *dq-axes* reference frame can be drawn as shown in Figure 6:

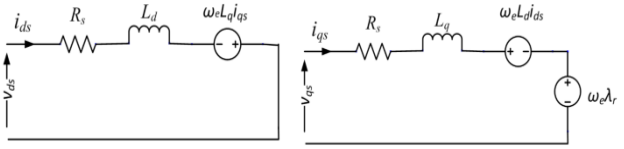

Figure.6. The *dq*-axes equivalent circuits of a AFPMSG in (consumer/load) notation

3-3 Power and torque analysis of a AFPMSG

According to assumptions, the electrical power input can be expressed in the *abc* reference frame as follows:

$P_{abc}=v_{as}i_{as}+v_{bs}i_{bs}+v_{cs}i_{cs}(14)$

Or in the *dq*-axes reference frame as follows:

$P_{dq}=\frac{3}{2}(v_{ds}i_{ds}+v_{qs}i_{qs})$ (15)

As a part of the input power, in the motoring mode, the active power is the power that is transformed to mechanical power by the machine, which can be expressed as follows:

$$P_{em}=\frac{3}{2}(e_d i_{ds}+e_q i_{qs}) \quad (16)$$

where, $e_d=-\omega_e L_q i_{qs}=-\omega_e\lambda_q$ (17)

and $e_q=\omega_e L_d i_{ds}+\omega_e\lambda_r=\omega_e\lambda_d$ (18)

Here, $e_d$ande_q , are the back EMFs in the *dq*-axes reference frame, and $\lambda_d$and $\lambda_q$are the*dq*-axes flux linkages. Substituting expressions (17) and (18) into (16), the active power can be re-expressed as follows:

$$P_{em}=\frac{3}{2}\omega_e(\lambda_d i_{qs}-\lambda_q i_{ds}) \quad (19)$$

Hence, the electromagnetic torque developed by a AFPMSG can be deduced as follows:

$T_e=\frac{P_{em}}{\omega_e/\frac{p}{2}}=\frac{3}{2}\left(\frac{p}{2}\right)(\lambda_d i_{qs}-\lambda_q i_{ds})$ (20)

Or$T_e=\frac{3}{2}\left(\frac{p}{2}\right)(\lambda_r i_{qs}+(L_d-L_q)i_{qs}i_{ds})(21)$

where, p is the number of poles in the machine.

Simulik model of the AFPMSG based on equations (10) to (21), is completed with the developed electromagnetic torque equation, are illustrated in Fig. 7:

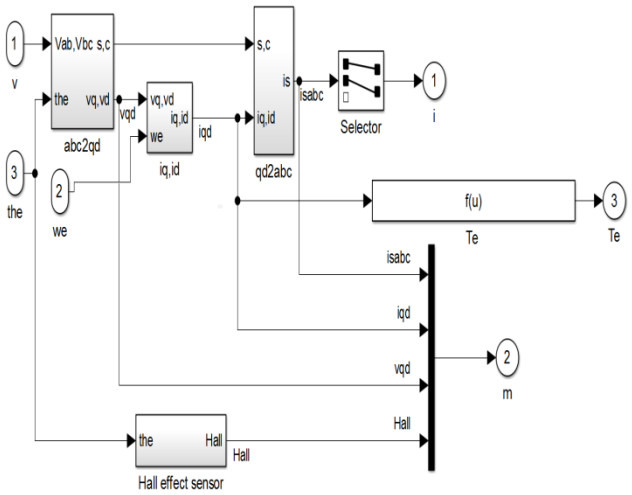

Figure.7. Dynamic model of the considered AFPMSG.

4. CONTROL OF GENERATOR-SIDE CONVERTER

In wind turbine AFPMSG systems, three system variables need to be strictly controlled [11]:
(1) The optimal power generated by the AFPMSG at different wind speed levels;
(2) The active and reactive power injected into the grid;
(3) The DC bus voltage of the back to back converter. Figure 8 shows a direct-drive wind turbine AFPMSG fed by a back-to-back converter. In this system, the generator-side converter regulates the speed of the AFPMSG to implement the MPPT control. Meanwhile, the grid-connected converter controls the active and reactive power injected into the grid.

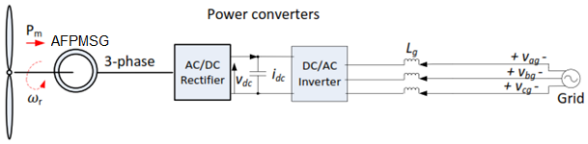

Figure.8. Direct-drive AFPMSG system

4-1 Maximum Power Point Tracking Control

Direct-drive AFPMSGs have the capability to work in a wide speed range. According to the intensity of the wind, the wind turbine generators need to be controlled to operate in three different modes as shown in Figure 9 [11]:

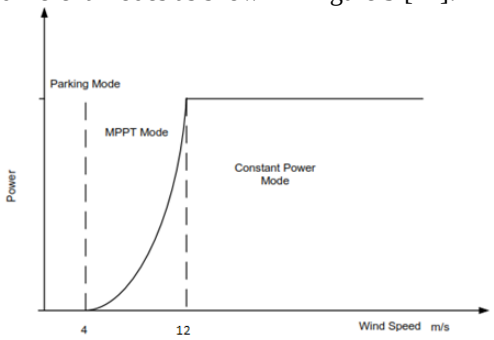

Figure.9. Wind turbine power-speed characteristic for the specific wind turbine

1. Parking Mode: when the wind speed is lower than the cut-in speed which is 4m/sec in this system, the wind turbine will not rotate but stay in parking status due to the fact that the electrical power generated by the AFPMSG system is insufficient to compensate for the internal power losses in this system. Therefore, the wind turbine is kept in parking mode by a mechanical brake;

2. MPPT mode: when the wind speed is greater than the cut-in speed, the wind turbine system starts to work and generate electrical power. Because the wind speed is in relatively low range in the MPPT mode, the power captured by the wind turbine is below its rated value, the MPPT control needs to be applied to ensure a maximum efficiency of power capture. The MPPT mode ends when the wind speed is greater than the rated wind speed, 12 m/sec, for this case-study system.

3. Constant power region: when the wind speed becomes greater than the rated value, the power generated by the system will be larger than its rated power if the MPPT control is still applied. This will increase the electrical stress on the AFPMSG and the power processing devices, and would further damage them. Therefore, the blade angle of the wind turbine blades needs to be properly controlled in the strong wind range to keep the system operating within its rated output condition. As its name implies, this is constant power region. As shown in equation (1), to control the captured mechanical power ,P_m ,at given wind speed, U_w , the only controllable term is the power coefficient,$C_p(\lambda)$. The power coefficient characteristic is shown in Figure 3. As can be seen in this figure, different power coefficient curves correspond to different blade angles. For each case, there is an optimal tip speed ratio, λ, which contributes to a peak power coefficient value which, in turn, leads to a maximum power capture,P_m . In the MPPT operation mode, the pitch angle is usually kept at zero degree.

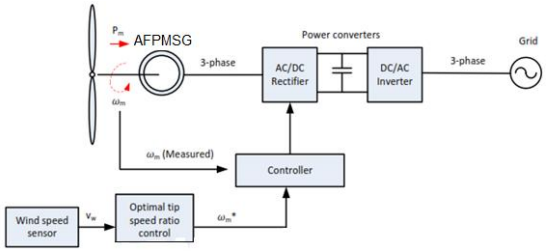

Figure.10. Tip speed ratio control scheme

In order to achieve the peak power coefficient value in the zero-degree pitch angle curve in Figure 3, the tip speed ratio needs to be controlled at the optimal value. From expression (1), the control of the tip speed ratio is actually the control of the rotor speed of the AFPMSG. A simplified scheme of tip speed ratio control is shown in Figure 10. From this figure, the wind speed information is sensed by a sensor and sent to a microcontroller, from which the reference speed of the AFPMSG can be calculated according to the optimal tip speed ratio. Consequently, the generator speed will reach its reference value in the static state, and then the MPPT control is achieved.

4-2 Field Oriented Control of the AFPMSG

The FOC approach was pioneered by F.Blaschke in 1970s [12].The FOC approach has been and continues to be a significant factor in AFPMSGs control. In the FOC approach, the *dq*-axes are rotating at the rotor electrical angular speed with the *d*-axis aligned with the rotor flux direction. Thus, the flux producing current component,i_{ds} , and the torque producing current component, i_{qs},are along the *d*-axis and *q*-axis, respectively. Thus, the *dq*-axes currents can be controlled independently by two closed loop controls in the FOC approach.
The FOC approach, although its implementation requires large computational effort including PI control and coordinate transformations, it possesses the following merits: (1) fast speed and torque response; (2) outstanding low speed performance; and (3) low current and torque ripples. For the application of direct-drive AFPMSG systems, the AFPMSGs are directly driven by the wind turbine without a gearbox, which means that their operation speeds are always in a relatively low range. Moreover, the torque ripples of the direct-drive AFPMSGs should be controlled at a low level to decrease the mechanical stresses on the wind turbine. On the basis of the analysis above, the FOC approach was found to be more suitable for the direct-drive AFPMSG systems. For a surface, mounted PM machine (SPM) which is applied in the case study system, the *d*-axis and

q-axis inductances are equal. Thus, the torque expression equation (21) can be simplified and rewritten as follows:

$$T_e = \frac{3}{2}\left(\frac{p}{2}\right)\lambda_r i_{qs} \quad (22)$$

In order to achieve the maximum torque per ampere, the d-axis current is set at zero. Thus, there will be a linear relationship between the electromagnetic torque and the q-axis current, such that the electromagnetic torque can be easily controlled by regulating the q-axis current. The phasor diagram for the FOC approach is shown in Figure 11, and the control scheme of the generator-side converter is shown in Figure 12.

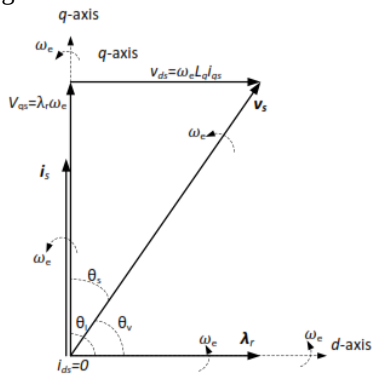

Figure.11. Phasor diagram of the FOC

As stated earlier, the FOC approach coupled to the optimal tip speed ratio based MPPT control strategy is applied here as the control algorithm for the generator-side power converter. In Figure 12, there are three feedback loops in the control system which are: (1) the speed control loop, (2) the d-axis current control loop, and (3) the q-axis current control loop. In the speed loop, at every sampling time, the actual speed of the generator sensed by an encoder mounted on the shaft of the rotor is compared to its reference value, which in turn is generated by the optimal tip speed ratio control, and then the error is sent to a PI controller which will output the reference q-axis current, meanwhile, the reference d-axis current, is always set at zero.

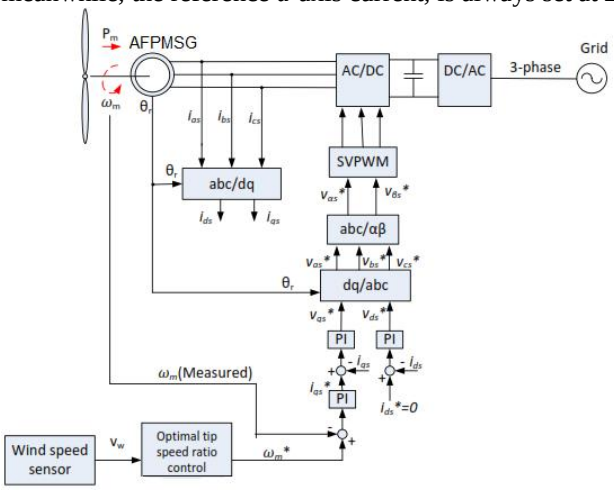

Figure.12. Generator-side control scheme

To acquire the feedback current signals, three-phase stator currents are sensed and transformed into the dq-axes reference frame according to Park's transformation. The reference stator voltages are then being achieved by PI controllers in the dq-axes current control loops. Here, the space vector pulse width modulation (SVPWM) approach is applied as the modulation strategy in this system, because it generates less harmonic distortion in the output stator voltages/currents and provides more efficient use of the DC supply voltages than the conventional sinusoidal pulse width modulation (SPWM). The outputs of the SVPWM model are six PWM signals to control the ON/OFF state of the six IGBT switches in the generator-side converter.

4-3 Simulation Results and Analysis

Simulation studies were carried out in MATLAB-Simulink to validate the chosen case-study system. The parameters of the case-study wind turbine and the associated AFPMSG are shown in Table 1. Figure 13 shows the control system diagram of the FOC approach built in Simulink.

Table.1. Electromechanical data of the considered AFPMSG.

Generator Type	AFPMSG
Rated Mechanical Power	600 W
Rated Rotor Speed	450 r/min
Rated Frequency	50 (Hz)
Number of phases	3
Number of Pole Pairs	8
Rated votage	300 v
Rated Mechanical Torque	8 Nm
Stator Winding Resistance	3.5 ohm
d axis Synchronous Inductance	8 mH
q axis Synchronous Inductance	8 mH
Wind Turbine Rotor Radius	3 m
IGBT Modulation Frequency	3 kHz

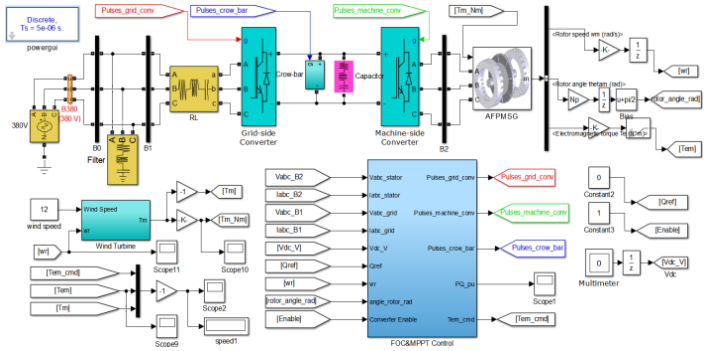

Figure.13. Control diagram of the system

Simulation results of the proposed system are shown in Figures 14 through 20.Figure 14 shows the wind speed input for the system. As can be seen in this figure, from0-1.3s, the wind speed increases from (cut-in speed) to and then is maintained constant at till 1.3s. In this wind speed range, we can investigate the performance of the proposed MPPT control strategy. From 1.3-2.6s, the wind speed increases from to (rated wind speed). In this wind speed range, the performance of the system in its rated condition can be evaluated. After that, the wind speed continues to increase to which exceeds its rated wind speed. Thus, the constant power control algorithm to deal with the high wind speed can be investigated. Shown in Figure 15 is the actual rotor speed in p.u. Figure16 shows the corresponding three-phase stator currents in p.u. The d-axis and q-axis currents are shown in Figure 17and Figure 18, respectively. Meanwhile, Figure 19 shows the electromagnetic torque developed by the generator. The electrical power developed by the generator is shown in Figure 20.

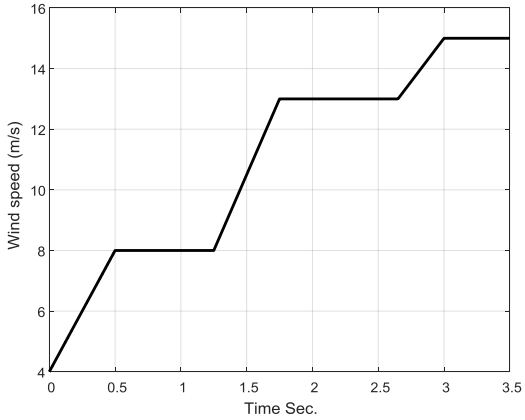

Figure.14. Wind speed input

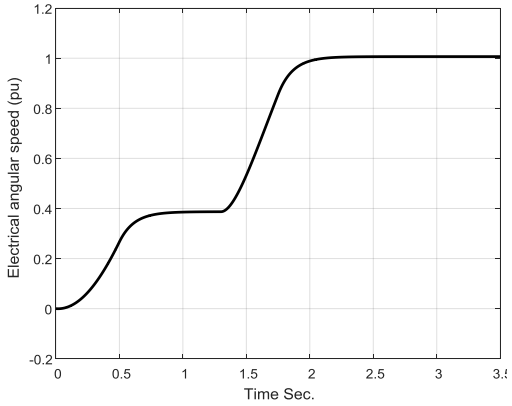

Figure.15. electrical angular speed of the AFPMSG in p.u.

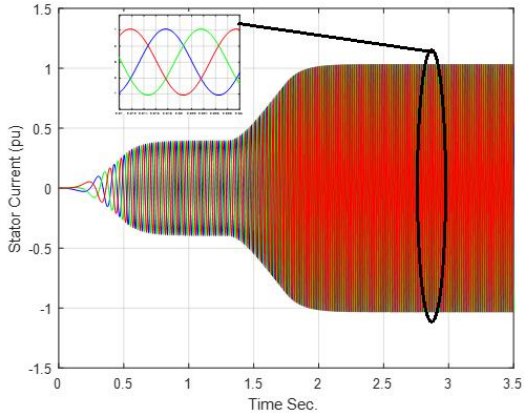

Figure.16. Three-phase stator currents in p.u

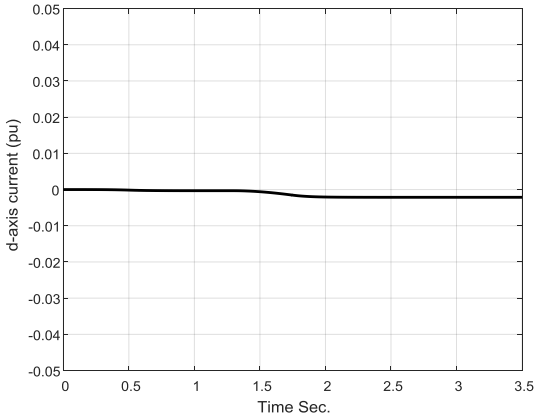

Figure.17.*d*-axis current in p.u.

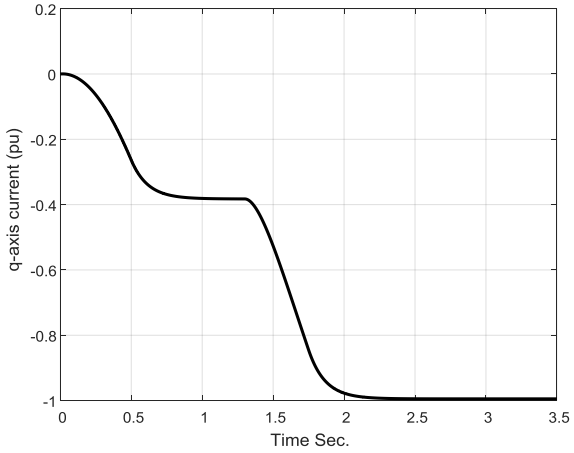

Figure.18.*q*-axis current of the inp.u.

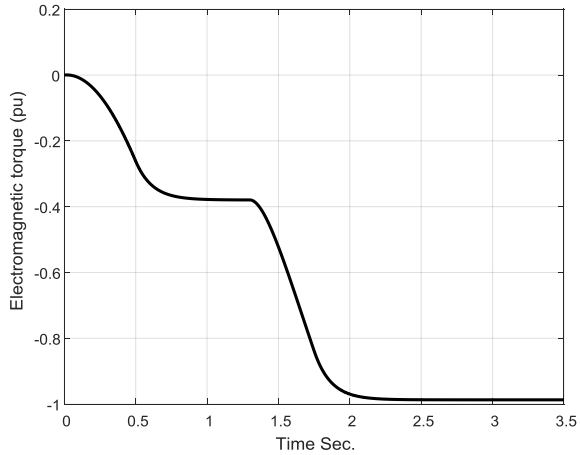

Figure.19. Electromagnetic torque in p.u.

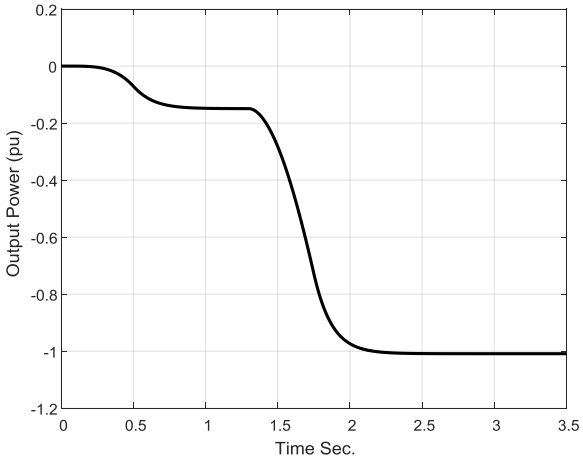

Figure.20. Electrical power generated in p.u.

As can be seen in the simulation results, according to different wind speed levels, the system performance has different characteristics best described as follows:

(1) From 0-1.3s: the wind speed starts to increase from the cut-in speed (4m/sec), which means that the generated electrical power is sufficient to compensate for the internal power consumption losses. Thus, the wind turbine begins to rotate and the AFPMSG begins to generate electrical power. As shown in Figures 15 through 20, with the increase of the wind speed, the stator currents, electromagnetic torque, and the generated electrical power are gradually increased. As can be seen in Figure 17, the *d*-axis current is controlled to be zero, which contributes to a

linear relationship between the *q*-axis current and the electromagnetic torque. From 0.5s, the wind speed reaches and stops increasing, soon after that the system comes to the steady state. (2) From 1.3-2.6s: starting from 1.3s, the wind speed increases from 8m/s to 12m/s ,which is the rated wind speed of the system. From 2.6-3.5s: the wind speed keeps increasing and exceeds the rated value. In order to limit the power input to prevent the electrical and mechanical stress on the system, the constant power control was applied in this wind speed range. That is, the mechanical power input of the system is kept at 1 p.u. and the generator speed is controlled at its rated value instead of increasing with the wind speed.

5. CONCLUSION

The paper proposes a AFPMSG -based variable speed wind energy conversion system with a simple MPPT control strategy based on the knowledge of the wind turbine characteristics. Based on the simulation results and the analysis above, optimal power is generated by the AFPMSG wind turbine system at different wind speed levels. The chosen control algorithms applied in the control system of the generator-side converter are hence verified. The control system was able to maximize the energy extracted from the wind as reflected from the power coefficients obtained during the simulation scenarios considered.

6. REFERENCES

[1].Soderlund, L., Koski, A., Vihriala, H., Eriksson, J-T., Perala, R., "Design of an Axial Flux Permanent Magnet Wind Power Generator", Eighth International Conference on Electrical Machines and Drives, (Conf. Publ. No. 444) , vol., no., pp.224,228, 1-3 Sep 1997.

[2].Chalmers, B.J., Wu, W., Spooner, E., "An Axial Flux Permanent Magnet Generator for a Gearless Wind Energy System", Proceedings of International Conference on Power Electronics, Drives and Energy Systems for Industrial Growth,vol.1, no., pp.610, 8-11 Jan 1996.

[3].S. Djebarri, J. F. Charpentier, F. Scuiller, and M. Benbouzid, "Design and Performance Analysis of Double Stator Axial Flux PM Generator for Rim Driven Marine Current Turbines," IEEE Journal of Oceanic Engineering, vol. 41, pp. 50-66, 2016.

[4].M. Aydin, S. Husang, and T. A. Lipo, "Optimum design and 3D finite element analysis of non-slotted and slotted internal rotor type axial flux PM disc machines", Power Engineering Society Summer Meeting, pp. 1409-1416, 2001.

[5].F. Caricchi, F. Crescimbini, O. Honorati, and E. Santini, "Performance evaluation of an axial flux PM generator", Proceedings of International Conference on Electrical Machines (ICEM) , pp. 761-765, 1992.

[6].R. J. Hill-Cottingham, P. C. Coles, J. F. Eastham, F. Profumo, A. Tenconi, G. Gianolio, "Multi-disc axial flux stratospheric propeller drive", Proc. of IEEE IAS Annual Meeting Conference Record 2001,vol. 3, pp. 1634-1639, 2001.

[7].U. K. Mirza, N. Ahmad, T. Majeed, and K. Harijan., "Wind energy development in Pakistan", Renewable and Sustainable Energy Reviews, Vol. 11, No. 9: pp.2179- 2190, 2007.

[8].Siegfried Heier. "Grid Integration of Wind Energy Conversion Systems", John Wiley & Sons Ltd, 1998, ISBN 0-471-97143-X, New York, USA.

[9].A. E. Fitgerald, J. C. Kingsley, and S. D. Umans, Electric Machinery. New York: McGraw-Hill, 1990.

[10].R. M. Park, "Two-reaction theory of synchronous machines, pt. I: Generalized method of analysis," AIEE Trans., vol. 48, pp. 716–730, July 1929.

[11].B. Wu, Y. Lang, N. Zargari, and S. Kouro, "Power Conversion and Control of WindEnergy Systems". Hoboken, NJ: Wiley, 2011.

[12]. Blaschke, Felix. "The principle of field orientation as applied to the new TRANSVECTOR closed loop control system for rotating field machines." Siemens review34, no.5 (1972): 217-220.